Comparison of Selectively Polarizable Force Fields for Ion−Water−Peptide Interactions: Ion Translocation in a Gramicidin-like Channel

Karen A. Duca[†,‡] and Peter C. Jordan[*,†,§]

Program in Biophysics and Department of Chemistry, Brandeis University, P.O. Box 9110, Waltham, Massachussetts 02454-9110

Received: April 24, 1998

Previous molecular dynamics simulations have shown that explicit inclusion of electronic polarizability significantly influences correlations in a gramicidin-like channel (ref 1). We now separately consider how water and helix polarization modify structure in the single-file regime of the head-to-head $\beta^{6.3}$ helix. Further, we investigate how internal energy barriers are influenced by polarization. We contrast midmonomer properties for small and large cations (Na^+ and Cs^+, respectively) and for four polarizability scenarios: all polar groups polarizable; only water polarizable; only helix groups polarizable; and no polar groups polarizable. To ensure comparability, the group dipole moments in nonpolarizable cases are adjusted to mimic either mean electrostatic interaction energetics or mean group dipole moments of the fully polarizable water-filled channel. With a polarizable helix, ion−carbonyl correlations strengthen and ion−water correlations weaken. With polarizable water, the opposite holds. The consequences of helix dipole fluctuations are quantitatively more significant. In examining coordination near the local energy extrema, we found that ion-specific differences in the energy barrier correlate with differences in translocation-induced changes in both ion−carbonyl and ion−water correlation. In traversing the local maximum, the number of carbonyl groups tightly solvating Cs^+ does not change, but for Na^+ the number increases by one. The shortest Na^+−water distance increases, while the corresponding Cs^+−water distance decreases. Polarizability influences barrier heights in much the same way it influences ion−water and water−water correlations. A polarizable helix tends to raise internal translocation barriers, as ion−carbonyl interactions are strengthened relative to ion−water interactions. Moreover, the water chain is disrupted by intercalating carbonyl groups. Polarizable water tends to lower barriers by enhancing ion−water and water−water interactions, which assist the ion in overcoming the barrier. Consequently, partial incorporation of polarizability may introduce larger errors into the simulation than completely neglecting this property.

Introduction

Cationic permeation through the gramicidin channel has been studied theoretically for the last 20 years. An early attempt involved a fixed, periodic, dipolar array[2] interacting with monovalent cations. The field progressed with studies of rigid channel analogues with and without water,[3,4] idealized β-helices,[5−7] and ultimately, right-handed dimers based on experimental NMR structures with many waters and a lipid-like domain.[8] Today molecular dynamics trajectories of several hundred nanoseconds employing full-atom peptide representation with solid-state NMR-derived coordinates, hundreds of waters, and explicit phospholipid are not impossible.[9] The trend has moved from simplified, abstract systems to sophisticated, "realistic" models. Despite the richness of the models currently in vogue, none has yet completely achieved accurate quantitative prediction of gramicidin's behavior.

In addition to ensuring that boundary conditions do not introduce spurious correlations and to treating long-range electrostatic effects adequately, analyses of complex systems require reliable force fields. This is especially true for ion channels, where selectivity rests on a delicate balancing between rather large energies in two quite distinct solvation environments: bulk water and the channel interior. Small errors in potential functions may result in seriously flawed qualitative and quantitative predictions.[10−14]

The field of an ion strongly polarizes nearby water and channel groups; the requirement of single-filing imposed on water by small channel radii and on channel groups by the protein backbone significantly influence the reorientation of these species in response to the ionic field.[15] This leads to strong local effects that are poorly described by standard biomolecular force fields such as CHARMM, GROMOS, or CVFF.[16−19] These (and other) commonly used force fields rely on pairwise, additive nonbonded interatomic potential energy functions that either completely neglect nonadditivity or only approximate it via an effective pairwise additive interaction term. Moreover, water features have been parametrized to account for structure and behavior in the liquid phase. Within the channel environment, however, where the structure and mean dipole moment of water differ dramatically, such approximations are not always appropriate.[1,20]

Investigators have recognized for some time that polarization may significantly influence channel energetics[4,7,20] and protein energetics generally.[21] To treat such phenomena in a compu-

* To whom correspondence should be addressed, at the Department of Chemistry, MS-015, Brandeis University. Fax (781) 736-2516, e-mail jordan@brandeis.edu.

† Program in Biophysics.

‡ Present address: Department of Chemical Engineering, University of Wisconsin, Madison, WI 53706, U.S.A.

§ Department of Chemistry.

10.1021/jp981995z CCC: $15.00
Published on Web 10/16/1998

tationally simpler way, Roux proposed a modification to the CHARMM force field that partially incorporated ion-induced polarization energy, E_{pol}, for ion−peptide interactions.[22] He treated as contributing to E_{pol} three interactions: between the ion and the induced dipoles, between the induced dipoles and helix partial charges, and among the induced dipoles. The ion−induced-dipole interaction contributes a pairwise additive term to the polarization energy, whereas the other two are nonadditive energy corrections. All three terms are first-order in atomic polarizability, α. This study differs from earlier work that treats polarization of both peptide and water to all orders in α.[1,4,7,20]

The polarizable peptide (partial inclusion of polarizability) approach was used to study single and double occupancy of gramicidin by all five common alkali cations[23] and to study Na^+ binding within a channel embedded in a fully hydrated dimyristoyl phosphatidylcholine bilayer.[24] Nonpolarizable TIP3P[24a] water was used in both simulations. The consistency of incorporating the influence of helix polarizability while excluding water polarizability is arguable and at some level physically unrealistic. Although these simulations provide an excellent window into the effects of helix polarizability and reproduce qualitatively many aspects of gramicidin structure/function, the calculated free energy profile is not completely in agreement with experimental findings, and the predicted location of the Na^+-binding site is shifted too far toward the bulk.[24] Woolf and Roux indicate[24] that a fully self-consistent treatment of polarization, such as was used in earlier studies,[4,7,20] is likely to be needed for an improved description of microscopic behavior and for a better match with experimental binding energies.

To assess in detail the consequences of partial inclusion of polarizability, we have studied the effects of selective incorporation of helix vs water polarizability on ion−water−helix structure in the midmonomer region of the head-to-head $\beta^{6.3}$ helix. For the channel, we used a fully hydrated, flexible, polyglycine analogue of gramicidin, with water in the capping domains and immobile, lipid-like force centers mimicking the effects of the bilayer leaflets.[1,20] We investigated how midmonomer energy barriers were influenced by polarization and studied the specific solvation associated with passage between two local extrema in the energy profile. We contrasted properties for cations of different radii, one small and the other similar to the channel radius, Na^+ and Cs^+, respectively, and the effects of four polarizability scenarios: all polar groups polarizable; only water polarizable; only helix groups polarizable; and no polar groups polarizable. In the case when water was nonpolarizable, we also examined the effects of using one (all water as bulklike) or two types of water (channel and bulklike). The purpose of using two types of nonpolarizable water is to more accurately reflect the vastly different environments of the channel and bulk regions, although only one type of water is used in standard biomolecular force fields.

To ensure comparability, we adjusted the group dipole moments in nonpolarizable cases to mimic either mean electrostatic interaction energetics or mean group dipoles of the fully polarizable, water-filled channel. The very low dipole moments that reflect mean electrostatic interaction energetics are physically unreasonable, as are simulations where only one component of the system is polarizable (helix or water). Nonetheless, the simulations provide a sensitivity analysis regarding the value of fixed dipole moments and an independent assessment of the nature and magnitude of helix vs water polarizability effects.

Our computations yielded structural data illustrating how cation identity and separately polarizable components modified the electrical properties of the channel groups, as well as ion−water, water−water, and ion−helix correlations, which collectively describe the ionic transport process across the membrane. In a particularly simple channel domain, the midmonomer, we calculated the potential of mean force (PMF) for Cs^+ and Na^+ and explored the origin of the differences in internal translocational barrier heights and ionic coordination attributable to partial incorporation of polarizability. Our results provide a cautionary tale with respect to how to include polarization in model force fields, and as such should be relevant to simulations of solvated proteins generally and to detailed study of phenomena at water−protein interfaces and within protein interiors in particular.

Model and Theory

Model System. The structure of the predominant ion-conducting form of gramicidin A in oriented bilayers has been elucidated by NMR spectroscopy.[25−29] The unified-atom model employed here, however, is a well-defined polyglycine analogue of the head-to-head dimer that incorporates major qualitative features essential to understanding the electrical conductance of gramicidin.[4,7,20,30,31] This model is also easily amenable to modification of basic group properties, such as individual group dipole moments, masses, or moments of inertia. Given gramicidin's narrow diameter and lack of interior side chains, the peptide carbonyl groups assume primary responsibility for the transport of ions through the pore. Consequently, models constructed to have a single amino acid with a simple radical group possess the most important molecular features governing ionic translocation and have been widely used.[7,20,32] Our model neglects any modulatory effects introduced by the specific geometry of the lipid environment or the side chains, modifications that can noticeably affect channel energetics.[33−35]

Conformational analysis provides a reasonable set of coordinates for the backbone atoms of the model dimeric channel.[36] The model is a left-handed structure, while gramicidin A is actually right-handed.[25−29] However, as the left- and right-handed versions of the polyglycine analogue are essentially equivalent, this choice has neither energetic nor structural consequences. Moreover, the channel is idealized for the purposes of (1) more easily comparing the effects of selective incorporation of group polarizability in the potential function and (2) evaluating the relative contributions that polarizability of peptide vs water groups makes to various structural and energetic properties. Handedness does not change the interpretation of our results in any way. In the structure we use, monomers are joined at the N-termini by means of 6 interhelical hydrogen bonds. Between the CHO group at the N-terminus and the COH of the ethanolamine tail are 15 carbonyl groups, all but 3 of which form intra- or intermonomer hydrogen bonds.

The complete model geometry is similar to that used previously,[1,20,37] with bulk water approximated by hemispherical caps of radius 11.5 Å at each end of the channel and containing ~40 water molecules each; the same damping algorithm was used to prevent water escaping the caps.[1] As described previously,[1] changing the cap radius from the 18 Å used originally[20,37] to 11.5 Å (and thus decreasing the number of waters from 418 to 44) had little effect on the PMF for Cs^+ in the single-file domain. The channel is again embedded in a lipid-like domain of 560 randomly distributed, immobile, nonpolarizable force centers occupying a cylindrical region (15 Å radius) around the model gramicidin dimer.[1,20,37]

Theory. The theoretical procedures used have been described in detail previously;[1,20,37] a brief outline will be presented here. Our emphasis in this study is on the consequences of selective

inclusion vs neglect of fluctuations in dipole moment. To do this, we compare three treatments that approximate the influence of bond polarization with computations that fully account for polarizability. We consider six distinct scenarios (denoted sc. in what follows): (sc. 1) all groups (i.e., CO, NH, and H_2O) have dipoles fixed at mean values with different values for channel and bulk water; (sc. 1A) the variant of sc. 1 in which channel and bulk water are assigned the same dipole moments; (sc. 2) channel water has dipoles fixed at a mean value lower than the bulk, whereas backbone groups are polarizable; (sc. 2A) the variant of sc. 2 in which channel and bulk water are assigned the same dipole moments; (sc. 3) helical backbone dipoles are fixed at mean values, whereas water is polarizable; and (sc. 4) all groups are polarizable.

We consider two ways of choosing effective dipole moments for the fixed (nonfluctuating) moment models. The more obvious is to fix the dipole moments at the average values (in debyes) obtained for fully polarizable simulations with use of an ion-free channel, thus attempting to mimic dipolar influences on mean local ordering. This approach yields the assignments: CO, 2.54 D; NH, 1.08 D; bulk H_2O, 2.47 D; channel H_2O, 2.31 D. We call this choice the high-μ_{eff} simulation category.

A completely different approach is to fix the moments at values that yield equivalent electrostatic contributions to the total energy. In a polarizable system the total electrostatic energy is:[4]

$$E_{\text{elec}} = {}^1/_2\, q_{\text{I}}\phi_{\text{I}} - {}^1/_2 \sum \vec{\boldsymbol{\mu}}_j \vec{\mathbf{E}}_j + {}^1/_2 \sum (\delta\vec{\boldsymbol{\mu}}_j)^2/\alpha_j \qquad (1)$$

with q_{I} the ionic charge; ϕ_{I} the electrical potential at the ion; $\vec{\boldsymbol{\mu}}_j$, $\delta\vec{\boldsymbol{\mu}}_j$, and $\vec{\boldsymbol{\mu}}_j{}^0$ the total dipole moment, the polarization contribution, and the bare dipole moment of group j, respectively; $\mathbf{E}_j$ the electric field at group j; and α_j the polarizability of group j. Since

$$\vec{\boldsymbol{\mu}}_j = \vec{\boldsymbol{\mu}}_j{}^0 + \alpha_j \mathbf{E}_j \equiv \vec{\boldsymbol{\mu}}_j{}^0 + \delta\vec{\boldsymbol{\mu}}_j \qquad (2)$$

the electrostatic energy can be rewritten as

$$E_{\text{elec}} = {}^1/_2\, q_{\text{I}}\phi_{\text{I}} - {}^1/_2 \sum \vec{\boldsymbol{\mu}}_j{}^0 \cdot \vec{\mathbf{E}}_j \qquad (3)$$

As

$$\phi_{\text{I}} = \sum \vec{\mathbf{V}}_{I_j} \vec{\boldsymbol{\mu}}_j \text{ and } \mathbf{E}_j = \vec{\mathbf{V}}_{I_j} + \sum{}' \vec{\mathbf{T}}_{jk} \vec{\boldsymbol{\mu}}_k \qquad (4)$$

where $\mathbf{V}$ is the charge-dipole vector, $\mathbf{T}$ is the dipole−dipole tensor, and the prime indicates that summation excludes the term $k = j$), then

$$\mathbf{V}_{j\text{I}} \equiv \mathbf{r}_{j\text{I}}/(\mathrm{r}_{j\text{I}})^3 \text{ and } \mathbf{T}_{jk} \equiv [3\mathbf{r}_{jk}\mathbf{r}_{jk}/(\mathrm{r}_{jk})^2 - \mathbf{I}]/(\mathrm{r}_{\text{jk}})^3 \qquad (5)$$

and the electrostatic energy can be expressed as

$$E_{\text{elec}} = q_{\text{I}} \sum (\vec{\boldsymbol{\mu}}_j{}^0 + {}^1/_2 \delta\vec{\boldsymbol{\mu}}_j) \cdot \vec{\mathbf{V}}_{\text{Ij}} - {}^1/_2 \sum{}' \vec{\boldsymbol{\mu}}_j{}^0 \cdot \mathbf{T}_{jk} \cdot \vec{\boldsymbol{\mu}}_k \qquad (6)$$

providing an energy-based definition for the effective equivalent dipole moments

$$E_{\text{elec}} = q_{\text{I}} \sum \vec{\boldsymbol{\mu}}_{j,\text{eff}} \cdot \vec{\mathbf{V}}_{\text{Ij}} - {}^1/_2 \sum{}' \vec{\boldsymbol{\mu}}_{j,\text{eff}} \cdot \vec{\mathbf{T}}_{jk} \cdot \vec{\boldsymbol{\mu}}_{k,\text{eff}} \qquad (7)$$

Comparing eqs (6) and (7) yields two possible identifications, indicative of the fact that there is no unique correspondence

$$\mu_{j,\text{eff}} \equiv {}^1/_2\, (\mu_j{}^0 + \mu_j) \text{ or } \mu_{j,\text{eff}} \equiv (\mu_j{}^0 \mu_j)^{1/2} \qquad (8)$$

The ion−dipole identification suggests that $\mu_{j,\text{eff}}$ is the arithmetic mean of the bare and mean dipole moments in the fluctuating dipole simulation; the dipole−dipole identification suggests a geometric averaging. Both assignments are heuristic since the time evolution of the orientations of the $\vec{\boldsymbol{\mu}}^0$, $\vec{\boldsymbol{\mu}}$, and $\vec{\boldsymbol{\mu}}_{\text{eff}}$ need not be (and almost certainly is not) identical. In either case, the effective moments are significantly less than the mean moments. Although the two identifications differ formally, in practice the values of $\mu_{j,\text{eff}}$ differ negligibly. Choosing the geometric mean (since the overwhelming majority of the interactions are dipole−dipole) yields the equivalencies: CO, 2.36 D; NH, 1.02 D; bulk H_2O, 2.14 D; channel H_2O, 2.07 D. We call this choice the low-μ_{eff} category.

In both treatments of the fixed dipole moments, we considered the effect of assigning different values to the channel and bulk waters because, as shown previously,[20] channel and bulk environments polarize water quite differently. Bulk water is far more effectively polarized and its mean dipole moment is larger. In sc. 1A and 2A, water dipoles are fixed at a single value (bulk H_2O), the approach used in standard biomolecular force fields. Our purpose here is to determine whether, in treatments ignoring polarization, the assumption that the force fields for bulk and channel water are equivalent has significant consequences.

As the ion is translated through the channel, umbrella-sampling links neighboring regions to generate an energy profile for the permeating ion.[38] The procedure is that used in earlier studies.[20] We started with a configuration located on one side of an energy maximum in midmonomer and moved the ion through the barrier and just beyond the adjacent local minimum. The total distance sampled along the z-axis for both Cs^+ and Na^+ was 1.6 Å with windows separated by 0.05 Å. Because the ions considered were relatively tightly tethered to their z-position (rarely moving more than 0.05 Å from the window center), overlap of the PMFs involved all bins that represented at least 5% of the total number of events sampled; typically 5 bins were included in the overlap, each containing at least 200 occupants. Because of the inherent uncertainty in the overlapping procedure and the large number of windows ($n = 32$), some error accumulation was unavoidable. We estimate the total uncertainty in the barrier heights obtained to be ∼0.2−0.3 kcal/mol.

To account for longer-range interactions, we used a cutoff of 12 Å, larger than the 9 Å used previously[1]; this too had little effect on midmonomer properties. Ion−water and ion−helix correlational properties for moieties within 9 Å of the ion were unaffected to within statistical error. Temperature control was maintained by Langevin coupling with a relaxation time of 0.1 ps.[39] A 5-point Gear predictor−corrector method was used to solve the equations of motion.[40] Rotational coordinates were described by Cayley−Klein parameters.[41] Moments of inertia were increased 10-fold for the polar groups of the helix, 100-fold for water. This slows the rate of water, CO, and NH rotation and facilitates rotational energy transfer, which can have no effect on equilibrium properties but permits use of relatively large time steps (2 fs) in the calculation, thereby reducing the computer time required.

The same starting configuration was used for each of the six scenarios with a given ionic occupancy. The channel was annealed for at least 10 ps at 400 K and 15 ps at 350 K, followed by at least 100 ps (but not more than 140 ps) of equilibration at 300 K. In each window the system was reequilibrated for 20 ps, and data were collected at 10-fs intervals for the next 40 ps. Channels containing only water were subjected to the same

TABLE 1: Polarizability Scenarios and Effective Dipole Moments of Nonpolarizable Groups (in Debye)[a]

polarizability scenario	CO	NH	H_2O channel	H_2O bulk
low μ_{eff}				
1	2.36	1.02	2.07	2.14
1A	2.36	1.02	2.14	2.14
2	fluctuating	fluctuating	2.07	2.14
2A	fluctuating	fluctuating	2.14	2.14
3	2.36	1.02	fluctuating	fluctuating
high μ_{eff}				
1	2.54	1.08	2.31	2.47
1A	2.54	1.08	2.47	2.47
2	fluctuating	fluctuating	2.31	2.47
2A	fluctuating	fluctuating	2.47	2.47
3	2.54	1.08	fluctuating	fluctuating
4	fluctuating	fluctuating	fluctuating	fluctuating

[a] Low μ_{eff} refers to effective dipole moments that reproduce equivalent electrostatic interaction energies; high μ_{eff} reflects the average dipole moments in water-only channel simulations with all groups polarizable (see text).

thermalization and equilibration procedure; however, without an ion to promote ordering, the system required longer annealing and equilibration times. The annealing times were 70 ps at the two high temperatures, followed by at least 150 ps for equilibration. Data were then collected for 250 ps. Given the simplified model and the number of constraints, these times were sufficient for equilibration of the system—as has been ascertained previously in two separate tests.[1]

Results

We contrasted properties of Cs^+-occupied, Na^+-occupied, and water-occupied channels under simulation conditions where polarization was selectively included in the potential function for (1) no species, (2) peptide CO and NH moieties only, (3) water only, and (4) both peptide groups and water. We also compared the effects of assigning different fixed dipole moments to channel and bulk water to reflect the very different environments that water encounters. Here we examine the six distinct scenarios defined in the theory section.

Scenarios 1−3 have some group(s) nonpolarizable. As described above, the effective dipole moments were chosen to mimic electrostatic interaction energies (designated low-μ_{eff}) or mean group-dipole values from a fully polarizable, water-filled channel simulation (designated high-μ_{eff}). Table 1 summarizes the features of the different polarizability scenarios. In contrast to our earlier study,[1] we can now independently analyze how water and peptide polarizability contribute to simulated system behavior.

We examined the structural and electrical properties of the single-filing channel waters, an internal energy barrier crossing in midmonomer, and ionic coordination as the ion was translated from a position just before a maximum in its essentially periodic energy landscape, then through and beyond the corresponding minimum. In reporting the effects of partial vs full incorporation of group polarizability on global channel properties and the cation-dependence of the observed differences, particular attention was paid to (1) ion−water and water−water correlations as a function of polarizability scenario; (2) the nature of ionic coordination at the maximum vs minimum and how that coordination correlates with ionic identity and group polarizability; and (3) trends in internal energy barriers as a function of selective incorporation of group polarizability and how they may reflect differential ionic solvation.

In all simulations the ion is started at ~5.60 Å from the dimer junction; in the final window it is near 7.20 Å. We classify as channel waters those molecules that remain within the channel for the entire duration of the simulation (in the so-called single-file regime) and do not exchange with bulk H_2O. The designation "near bulk" refers to water molecules whose z-coordinate is >14.0 Å but <15.0 Å from the dimer junction and which maintain contact with channel water on one side and bulk on the other. Near-bulk waters exchange readily with the bulk, which has no direct contact with interior channel water. At the extremities of the channel (~11.0 Å from the junction), the last channel water molecule switches places more or less frequently with a near-bulk H_2O, depending on (1) the occupancy (cation vs water-only) and (2) the polarizability scenario. These exchangeable molecules, which are sometimes channel water, sometimes near-bulk water, are excluded from our analysis.

Electrical Properties of Water and Peptide Groups. *Water Dipole Moments.* Table 2 and Figure 1 present the mean water dipole moments ($\langle\mu_w\rangle$) of those water molecules that are cotransported with the ion as it moves across an energy barrier in midmonomer. Values for equivalent water-only channels are also included in Table 2 for comparison. Water dipole moments are fixed at the indicated assigned values for sc. 1 and 2, but fluctuate in response to electric fields in sc. 3 and 4.

Some clear patterns emerge. In all ion-occupied channels, fixing the backbone groups' dipoles at mean values (sc. 3) results in higher $\langle\mu_w\rangle$. The opposite effect is observed for water in ion-free channels, but the magnitude of the difference is much smaller. For the ion-occupied channels, the $\langle\mu_w\rangle$'s in the high-μ_{eff} simulations are slightly smaller than those in low-μ_{eff} studies (although the difference may not be significant). This is not surprising, for the higher dipole moments of the helix groups allow the backbone to interact more strongly with both the ion and the channel waters, thereby creating competition with the ion−water interaction and reducing the average water dipole moments.

Figure 1 presents $\langle\mu_w\rangle$ for each single-file water as a function of polarizability scenario. Naturally, the largest values of $\langle\mu_w\rangle$ are for waters closest to the ion; $\langle\mu_w\rangle$ decreases quickly as the ion−water distance grows. The effective dipole treatment (sc. 1) provides a poor description of channel water dipoles. The low μ_{eff} assignment is always much less than $\langle\mu_w\rangle$ at any point in the single file. The high-μ_{eff} value is somewhat more satisfactory. However, $\langle\mu_w\rangle$ values near the ion are poorly approximated by either fixed value. Importantly, fixed water dipole moments present a static picture across the channel. The most closely coordinating waters, which are arguably critically important in assisting the ion over the translocation barrier, are poorly described by the force fields when mean values are used to describe the water dipoles within the channel. The highest $\langle\mu_w\rangle$ values are found when the backbone dipoles are fixed and water is polarizable. Allowing helix group dipoles to fluctuate lowers $\langle\mu_w\rangle$ most clearly for those waters closest to the ion (compare sc. 3 and 4).

In summary, the choice of polarizable vs nonpolarizable groups has a measurable effect on water dipole moments. Keeping the helix group dipole moments fixed raises $\langle\mu_w\rangle$ with respect to the matched scenario, in which the helix groups are polarizable. The obvious fact that waters closest to the ion are more highly polarized by the electric field of the ion (an effect whose strength is related to cation identity) cannot be adequately

TABLE 2: Mean Channel Water Dipole Moments in the Vicinity of the Ion (in debye)[a]

polarizability scenario	cesium		sodium		water,
	$\mu_{water\ 1}$	$\mu_{water\ 2}$	$\mu_{water\ 1}$	$\mu_{water\ 2}$	$\mu_{average}$
low μ_{eff}					
1	2.07	2.07	2.07	2.07	2.07
1A	2.14	2.14	2.14	2.14	2.14
2	2.07	2.07	2.07	2.07	2.07
2A	2.14	2.14	2.14	2.14	2.14
3	2.67 ± 0.03	2.47 ± 0.03	3.00 ± 0.03	2.61 ± 0.06	2.26 ± 0.04
4	2.52 ± 0.07	2.40 ± 0.02	2.83 ± 0.05	2.50 ± 0.08	2.32 ± 0.04
high μ_{eff}					
1	2.31	2.31	2.31	2.31	2.31
1A	2.47	2.47	2.47	2.47	2.47
2	2.31	2.31	2.31	2.31	2.31
2A	2.47	2.47	2.47	2.47	2.47
3	2.64 ± 0.05	2.45 ± 0.03	2.98 ± 0.03	2.59 ± 0.07	2.27 ± 0.03
4	2.52 ± 0.07	2.40 ± 0.02	2.83 ± 0.05	2.50 ± 0.08	2.32 ± 0.04

[a] Window-averaged dipole moments for the first ($\mu_{water\ 1}$) and second ($\mu_{water\ 2}$) nearest neighbor water molecules. $\mu_{average}$ is the dipole moment obtained from water-only channel simulations. Sc. 4 is repeated in both low- and high-μ_{eff} categories for ease of comparison.

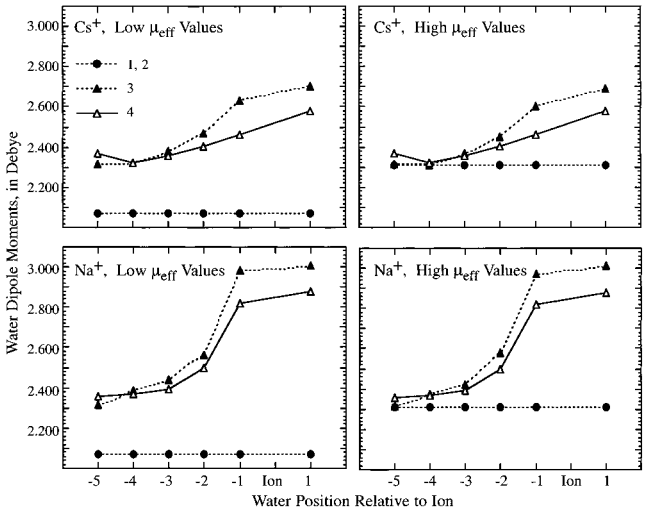

Figure 1. Mean water dipole moments as functions of polarizability scenario (in debye). The positive numbers along the *x*-axis refer to water molecules preceding the ion in the channel; the negative numbers indicate trailing waters. In sc. 1 and 2, μ_{water} is fixed.

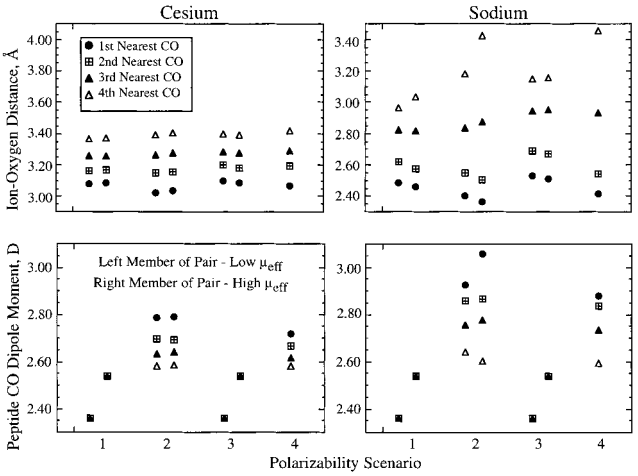

Figure 2. Ion−backbone carbonyl separations (in Å) and helix carbonyl group dipole moments (in Debye) for the four CO groups nearest the ion. The window-average ion−CO oxygen distance computed for all scenarios as the ion crosses an internal translocation barrier in the midmonomer (top panels). The corresponding helix dipole moments are given in the bottom panels. The ion-induced CO dipoles are uniformly higher than the fixed values assigned to backbone groups in the nonpolarizable scenarios. Root mean square (RMS) fluctuation: ∼0.05−0.10 Å for distances and ∼0.03−0.09 D for dipole moments.

described by models in which water is nonpolarizable, yet this fact is certainly relevant to quantitatively accurate channel description.

Peptide CO Dipole Moments. Figure 2 (bottom panels) presents mean dipole moments $\langle\mu_{CO}\rangle$ for the four carbonyl groups closest to the ion, averaged over all windows between the maximum and minimum. The left member of the pair for each polarizability scenario represents low-μ_{eff}, the right member, high-μ_{eff}. Note that the identity of the particular carbonyl groups included in the average actually changes (more or less frequently, depending on the polarizability scenario) as the ion moves through the channel.

For both ions, the dipole moments of the CO groups proximal to the ion considerably exceed the average values for the fixed scenarios. For cesium, $\langle\mu_{CO}\rangle$ ranges from ∼2.80 D for the closest CO to 2.60 D for the fourth closest, whereas the fixed average values are either 2.36 or 2.54 D. For sodium, the difference is even more pronounced, with $\langle\mu_{CO}\rangle$ ranging from ∼3.00 D to ∼2.60 D. Fixing water dipoles at average values with backbone groups polarizable (sc. 2) tends to broaden the distribution of CO moments for both ions compared with those in the fully polarizable sc. 4.

In summary, polarizable helix groups raise $\langle\mu_{CO}\rangle$ in the immediate vicinity of the ion. As with the water dipoles, assigned mean values fail to reflect local behavior induced by a transiting ion. When water groups are also polarizable, the two most closely coordinated CO dipole moments decrease slightly, as the two nearest waters now interact more strongly with the ion, whereas the dipole moments of those further away do not change significantly. These are small effects consistent with other trends.

Ion−Water and Ion−Backbone Interactions. *Ion−Water Correlations.* Table 3 summarizes data on window-averaged ion−water separations in the region between the maximum and minimum. For both Cs^+ and Na^+, the ion−water distances are shortest when channel waters are polarizable (sc. 3 and 4). For cesium ion−water, distances are largest when the backbone groups are polarizable and water is not (sc. 2). In sodium-occupied channels, the effect of backbone group polarizability is smaller and in the opposite direction. Although clear, these trends may be statistically insignificant.

Ion−water distances for the models in which channel waters are assigned dipole moments different from those of bulk waters (sc. 1 and 2) are slightly longer than if all waters are presumed to be equivalent (sc. 1A and 2A); differences are clearest for

TABLE 3: Mean Ion−Water, Water−Water, and $Water_1$−$Water_5$ Separations for Ion-Occupied Channels (in Å)

	cesium			sodium		
polarizability scenario	ion−water distance	water−water distance[a]	water chain length[b]	ion−water distance	water−water distance[a]	water chain length[b]
low μ_{eff}						
1	3.20 ± 0.03	3.16 ± 0.04	12.57 ± 0.14	2.60 ± 0.03	3.17 ± 0.06	12.62 ± 0.24
1A	3.19 ± 0.03	3.14 ± 0.04	12.49 ± 0.12	2.59 ± 0.03	3.16 ± 0.05	12.56 ± 0.23
2	3.22 ± 0.04	3.17 ± 0.08	12.66 ± 0.28	2.58 ± 0.03	3.17 ± 0.09	12.69 ± 0.28
2A	3.22 ± 0.04	3.17 ± 0.05	12.62 ± 0.15	2.58 ± 0.04	3.17 ± 0.05	12.65 ± 0.16
3	3.13 ± 0.05	3.07 ± 0.06	12.21 ± 0.13	2.50 ± 0.02	3.00 ± 0.09	12.01 ± 0.24
4	3.17 ± 0.05	3.11 ± 0.04	12.41 ± 0.13	2.50 ± 0.03	3.06 ± 0.10	12.28 ± 0.32
high μ_{eff}						
1	3.17 ± 0.04	3.11 ± 0.05	12.38 ± 0.14	2.57 ± 0.03	3.10 ± 0.07	12.42 ± 0.21
1A	3.15 ± 0.03	3.07 ± 0.04	12.22 ± 0.12	2.55 ± 0.02	3.06 ± 0.07	12.26 ± 0.22
2	3.20 ± 0.07	3.13 ± 0.07	12.49 ± 0.25	2.56 ± 0.03	3.11 ± 0.06	12.44 ± 0.21
2A	3.18 ± 0.04	3.10 ± 0.06	12.35 ± 0.15	2.54 ± 0.03	3.10 ± 0.07	12.35 ± 0.21
3	3.13 ± 0.04	3.10 ± 0.06	12.31 ± 0.17	2.50 ± 0.02	3.03 ± 0.10	12.17 ± 0.23
4	3.17 ± 0.05	3.11 ± 0.04	12.41 ± 0.13	2.50 ± 0.03	3.06 ± 0.10	12.28 ± 0.32

[a] Water−water distance refers to a complete average over all adjacent waters. [b] The water chain length represents the full length of the nonexchangeable, single-file regime.

the high-μ_{eff} case. In sc. 1 and 2, the ion−water distances are shorter for high μ_{eff} than for low-μ_{eff}. In sc. 3 no such differences are observed.

To summarize, ion−water separations are sensitive to the polarizability scenario. Having polarizable water tends to shorten ion-first water distances for both ions, whereas polarizable backbone groups tend to lengthen them for cesium but shorten them for sodium. Beyond the first water, ion−water interactions weaken for both ions when backbone groups are polarizable.

Ion−Peptide Carbonyl Group Correlations. Figure 2 (top panels) illustrates the average ion−carbonyl oxygen distances across all windows. All distances are fairly insensitive to variation of μ_{eff}. For cesium, which remains closer to the channel axis than sodium, mean ion−oxygen distances for the four solvating carbonyl groups are nearly independent of polarizability scenario. With the backbone groups polarizable and water not (sc. 2), the first and second carbonyls approach the ion more closely than in any other case, the third and fourth COs being somewhat more distant. With all groups polarizable (sc. 4), CO behavior is intermediate between "water-polarizable" and "helix polarizable" but is closer to the latter.

Sodium is somewhat different. Since it can move further off-axis, there is a relatively large gap between the first pair and second pair of ion−CO oxygen distances; this is particularly apparent when the helix group dipoles fluctuate (sc. 2 and 4). The case of fixed water dipoles and polarizable backbones (sc. 2) exhibits the closest approach between the ion and first two solvating carbonyl ligands, followed by sc. 4, in which all groups are polarizable.

To summarize, ion−carbonyl correlations are influenced by incorporation of polarizable groups for both ions but much more so for sodium. In general, backbone-only polarizability leads to closer coordination of the nearest two COs, whereas the next two COs are less well coordinated (compare sc.2 with sc. 1 and sc. 4 with sc. 3). Permitting water dipoles to fluctuate increases all ion−carbonyl distances (sc. 3 vs sc. 1 and sc. 4 vs sc. 2). Full polarizability is intermediate to backbone-only and water-only polarizability but is closer to the backbone-only case.

Water−Water Correlations and Ion-Induced Electrostriction. Several aspects of water−water interactions are notably dependent on explicit incorporation of polarizability. Table 3 presents an overview of channel average water−water separations, as well as the average water chain length from $water_1$ (immediately adjacent to the ion) to $water_5$ (the last nonexchangeable channel water). In the absence of explicitly polarizable water, the water−water distances for both cesium and sodium are roughly similar (sc. 1 and 2). When water is polarizable (sc. 3 and 4), the water−water distances are much shorter when sodium occupies the channel. Polarizability of helix backbone groups causes water−water distances, as well as total water chain length, to increase for both ions. Having only one vs two types of water (with the larger dipole moment) reduces water−water distances in all cases, although in some instances the differences are small, being noticeable only in overall chain lengths.

Allowing water dipoles to fluctuate (sc. 3 and 4) shortens the mean water−water separations relative to comparable fixed water dipole scenarios (sc. 1 and 2), with two exceptions: Scenarios 1A and 2A, high-μ_{eff} exhibit unusually small water−water separations for cesium occupancy. In these cases, the fixed water dipole is 2.47 D, larger than the ion induced values for all but the water immediately adjacent to the ion in sc. 3 and 4 (see Figure 1). The total water chain length is also correspondingly shorter. Both observations clearly suggest the inappropriateness of assuming that channel and bulk water can be described by the same (bulklike) fixed point-charge models. This demonstrates the importance of a polarizable water model in channel simulations since charge distributions of such model waters naturally respond differently in different solvation environments. The water−water distances are shorter in sc. 3 than in sc. 4, since the nonpolarizable helix dipoles do not interact as strongly with the water chain.

There is some degree of electrostriction (ion-induced shortening of water−water distances) for all ion-occupied channels in comparison with equivalent water-only channels, except in sc. 2, low μ_{eff} (see Table 4). This reflects the very low dipole moment value assigned to channel water molecules; with such low water dipole moments, the ion interacts preferentially with the helix backbone groups. Ion-induced electrostriction is most noticeable for sc. 3, where only water is polarizable, and then by the fully polarizable sc. 4.

Increasing the μ_{eff} has two basic effects: shortening water−water separations (as compared with low-μ_{eff} results) in all cases except for sc. 3, and augmenting electrostriction in comparison with the ion-free channel. The explanation for the anomaly in sc. 3 is that the nonpolarizable backbone groups (with their high, fixed dipole moments) now compete more effectively in interaction with the water chain. We conclude that water−water

TABLE 4: Channel Average Group Dipole Moments, Water−Water Distances, and the Mean Angle between the Water Dipole Moment Vector and the Channel Axis for Water-Filled Channels[a]

polarizability scenario	dipole moment, D				H_2O-H_2O distances, Å	$\theta_{average}$, deg
	$\mu_{channel}-H_2O$	μ_{bulk}[a]$-H_2O$	$\mu_{peptide}-CO$	$\mu_{peptide}-NH$		
low μ_{eff}						
1	2.07	2.14	2.36	1.02	3.20 ± 0.08	90 ± >30
1A	2.14	2.14	2.36	1.02	3.18 ± 0.06	92 ± >30
2	2.07	2.14	2.55 ± 0.05	1.07 ± 0.04	3.16 ± 0.05	86 ± >30
2A	2.14	2.14	2.55 ± 0.05	1.07 ± 0.04	3.19 ± 0.07	87 ± >30
3	2.26 ± 0.04	2.43 ± 0.12	2.36	1.02	3.14 ± 0.06	86 ± >30
4	2.32 ± 0.04	2.43 ± 0.10	2.56 ± 0.06	1.07 ± 0.05	3.12 ± 0.08	87 ± >30
high μ_{eff}						
1	2.31	2.47	2.54	1.08	3.13 ± 0.06	87 ± >30
1A	2.47	2.47	2.54	1.08	3.11 ± 0.06	94 ± >30
2	2.31	2.47	2.56 ± 0.06	1.08 ± 0.05	3.14 ± 0.07	87 ± >30
2A	2.47	2.47	2.56 ± 0.06	1.08 ± 0.05	3.12 ± 0.08	84 ± >30
3	2.27 ± 0.03	2.43 ± 0.10	2.54	1.08	3.17 ± 0.08	91 ± >30
4	2.32 ± 0.04	2.43 ± 0.10	2.56 ± 0.06	1.07 ± 0.05	3.12 ± 0.08	87 ± >30

[a] μ_{bulk} refers to the "near bulk" in contact with both channel and bulk waters (see text).

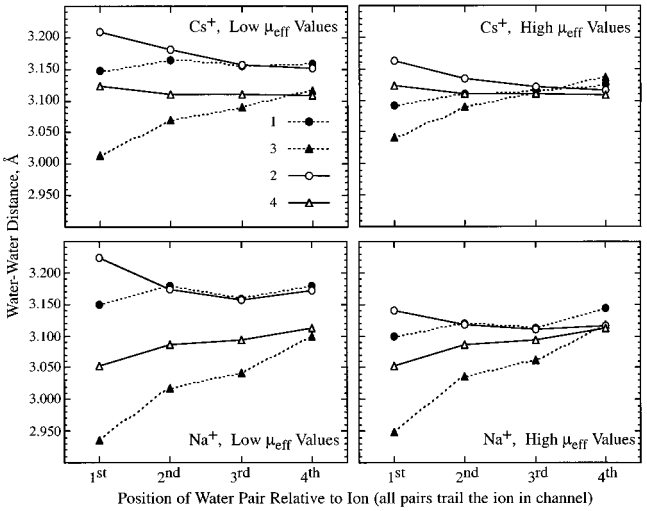

Figure 3. Water−water separations relative to the ion in the channel (in Å) as a function of polarizability scenario. Water−water distances are larger when helix dipoles fluctuate and smaller when water is polarizable. Water−water distances track fairly closely (although not exactly) the magnitude of the dipole moment vector.

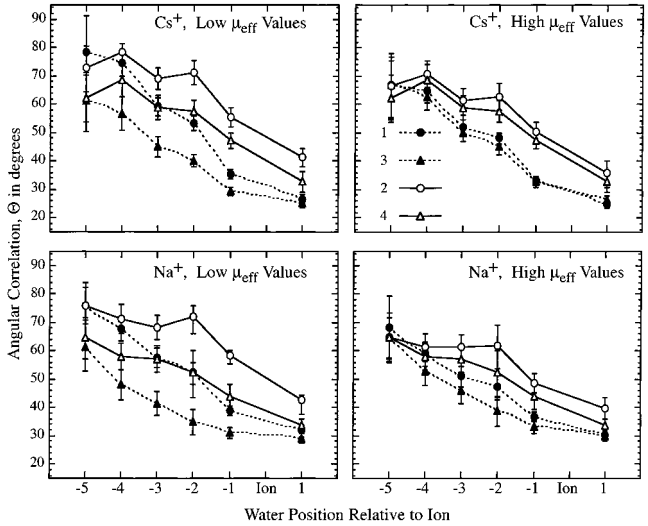

Figure 4. Dipolar orientation as a function of water location relative to the ion. The *x*-axis designates the position of water molecules. The ion is at zero; negative values represent the water molecules trailing the ion; and positive values indicate the water preceding the ion. The *y*-axis is the angle (in degrees) between the water dipole moment and the channel axis. Solid lines are polarizable backbone scenarios; dashed lines are fixed-backbone dipole moment scenarios. Each point shows the channel-averaged value. 0° orientation indicates perfect alignment; 90° denotes complete loss of correlation.

separations throughout the channel essentially reflect the magnitude of the water dipole moments (see Figure 3).

To summarize, channel average water−water separations, single-file water chain lengths, and location-specific water−water pair distances are all strongly influenced by partial or complete incorporation of polarizability. Polarizable water tends to strengthen water−water correlations, thereby reducing water−water distances, both adjacent to and more distant from the ion. Polarizable helix groups tend to weaken water−water correlations by interacting more strongly with the ion, as well as by directly disrupting the water chain. Assuming that channel water and bulk water are equivalent can yield anomalous predictions, indicating the inappropriateness of such an assignment. None of the approximate polarizability scenarios adequately describes the fully polarizable case, sc. 4.

Water Orientational Correlations. Orientational correlation is conceivably an important means by which information is communicated across the channel. Figure 4 illustrates the effects of group polarizability on orientational correlations in the water chain for an ion crossing an internal barrier in midmonomer.

As expected, orientational correlation is always highest close to the ion and is lost as the ion−water distance increases. In the water-filled channel, there is effectively no orientational correlation of water molecules under any simulation conditions (see Table 4). With an ion in the channel, a comparison of the polarizability scenarios shows that when helix group dipoles fluctuate (sc. 2 and 4), overall orientational correlation is less than in matched simulations where dipoles are fixed at average values (sc. 1 and 3). This is observed for both ions regardless of μ_{eff}, although the differences are smaller for high μ_{eff}.

Among the scenarios with fluctuating backbone dipoles, sc. 4 displays more long-range correlation, because the water is polarizable and water−water interactions are strengthened relative to carbonyl−water interactions. In all cases sc. 3 exhibits the most long-range orientational correlation. The reason is clear: Relatively strong water dipoles augment correlation; relatively weak helix dipoles have less disorienting capacity; and correlation is lost most rapidly for low μ_{eff}.

To summarize, making backbone groups polarizable weakens the propagation of dipolar correlations measured by water dipole orientations. The effect is somewhat more prominent for cesium, although polarizable water counteracts this tendency.

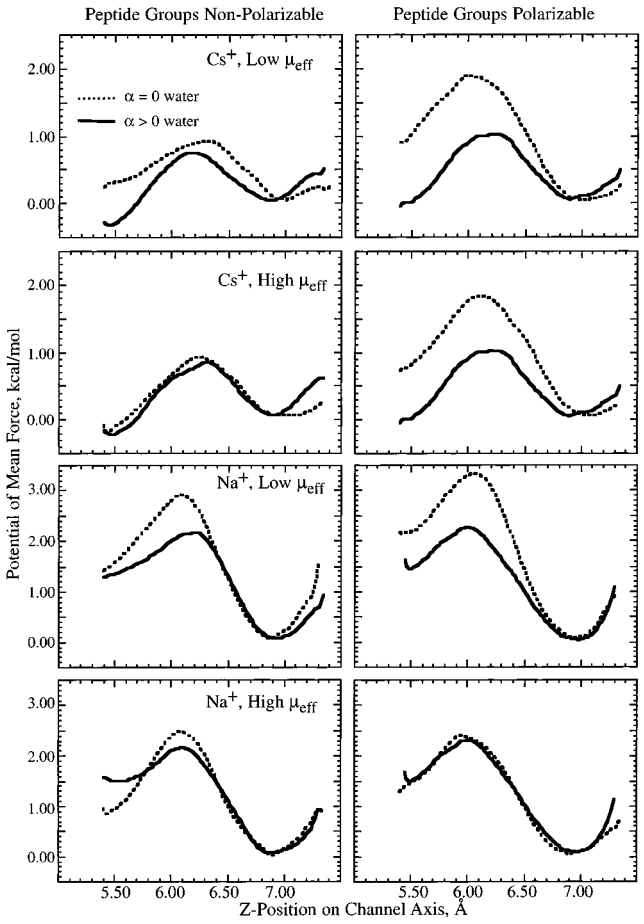

Figure 5. Internal translocation barriers as functions of polarizability scenario. Potential of mean force (PMF) for Cs^+ and Na^+ for each polarizability scenario at low and high μ_{eff}. Curves shown have been smoothed (five-point smoothing function). Statistical error in barrier heights, ~0.2−0.3 kcal/mol. Left-hand panels compare sc. 1 & 3; right-hand panels, sc. 2 & 4. Solid lines refer to polarizable water (sc. 3 & 4); dotted ones, nonpolarizable water (sc. 1 & 2).

This counteraction is, however, attributable to the high water dipole moments, as opposed to polarizable water per se. High water dipole moments encourage the propagation of long-range correlation by strengthening ion−water and water−water interactions relative to ion−carbonyl and carbonyl−water interactions. The greatest long-range correlation is observed for low mean backbone dipole moments (sc. 1 and 3). The fully polarizable sc. 4 is, on balance, most closely approximated by the nonpolarizable case, sc. 1.

Energetics of Internal Barrier Crossing. Previous theoretical treatments of the gramicidin channel suggest midmonomer energy barriers of between 1 and 5 kcal/mol, depending on the cation.[7,8,20,42] Figure 5 presents approximate PMFs computed for the various polarizability scenarios. Previous studies (unpublished results) compared the results of simulations performed for channels with all groups polarizable (sc. 4) and with no groups polarizable (sc. 1). In those studies, incorporating polarizability increased the internal translocation barrier for cesium but decreased it for sodium. The present study extends and clarifies this preliminary observation.

For both ions, barrier heights tend to drop when water polarizability is incorporated in the potential function, relative to equivalent nonpolarizable scenarios (compare sc. 1 and 3 or sc. 2 and 4). Incorporating polarizability for backbone groups generally tends to raise barrier heights (compare sc. 1 and 2 or sc. 3 and 4). Conversely, having water polarizable tends to lower the barrier heights.

The energy gap between sc. 2 and 4 is larger for cesium than for sodium and is also larger when μ_{eff} is low. Since the statistical uncertainty in barrier heights is ~0.2 kcal/mol, the differences in internal energy barriers may not be statistically significant. However, the trends resulting from selective incorporation of group polarizability are consistent.

Significantly, the low-μ_{eff} scenarios, while designed to mimic mean polarization energetics, always lead to higher internal translocation barriers. The most unreliable approximation appears to be polarizable peptide but nonpolarizable water (sc. 2). Because backbone and water polarization interfere destructively with respect to ion−water correlation, sc. 1 and 4 are energetically most similar.

To summarize, the PMF trends parallel those found for ion−water, ion−peptide, and water−water correlations. Barriers are generally larger when the peptide backbone dipoles fluctuate. Making water polarizable reduces the barrier; consequently, the smallest barriers arise when peptide dipoles are fixed at average values but water dipoles are allowed to fluctuate. With all groups polarizable, the larger barriers, which result from enhanced ion−carbonyl interactions, are counterbalanced by stronger water−ion and water−water interactions; the effect is more pronounced for sodium than for cesium.

Ionic Coordination at Extrema. We now turn to ionic coordination at the extrema and analyze the distribution of ion−carbonyl and ion−water distances: (1) to identify coordination patterns associated with the various polarizability scenarios, and (2) to determine whether scenario-specific coordination differences at extrema correlate with trends in internal barrier heights. Ion−water and ion−carbonyl oxygen distances from the three windows at and adjacent to an extremum were pooled, binned, and normalized. Data describing ion−CO behavior are presented in Figures 6 and 7. In moving between extrema, two of the carbonyls in the coordination shell are exchanged for two others, while one pair of carbonyls solvates the ion at both maximum and minimum.

The vertical dotted lines in Figure 6 define close CO coordination, a region of tighter binding, essentially the maximum in the first coordination shell. We compare integrated areas of the distributions to identify changes that might correlate with the variability in barrier heights. The overall degree of coordination at both extrema is similar for cesium, although the distribution is broadened at the energy maximum. Introducing backbone polarizability slightly increases the amount of close CO coordination at the minimum (~8% increase) while marginally decreasing it at the maximum. The effect of making water polarizable is to reduce the close CO coordination (sc. 3 vs 1 or sc. 4 vs 2), but only very slightly.

Although there is less overall close CO coordination for sodium (since sodium binds off-axis), scenario-specific differences in the sodium-occupied channel are more striking. Unlike cesium, sodium is better coordinated at the minimum. The shift in the overall coordination at the maximum to larger ion−oxygen distances is less pronounced. At both extrema, binding to the CO groups is tighter when peptide groups are polarizable (the peaks move inward). At the maximum, close CO coordination (the area in the region to the left of the vertical dashed line in Figure 6) increases by ~49%, whereas at the minimum it increases by ~75% relative to comparable simulations in which the peptide groups are nonpolarizable. Close CO coordination when water is polarizable is reduced from that for

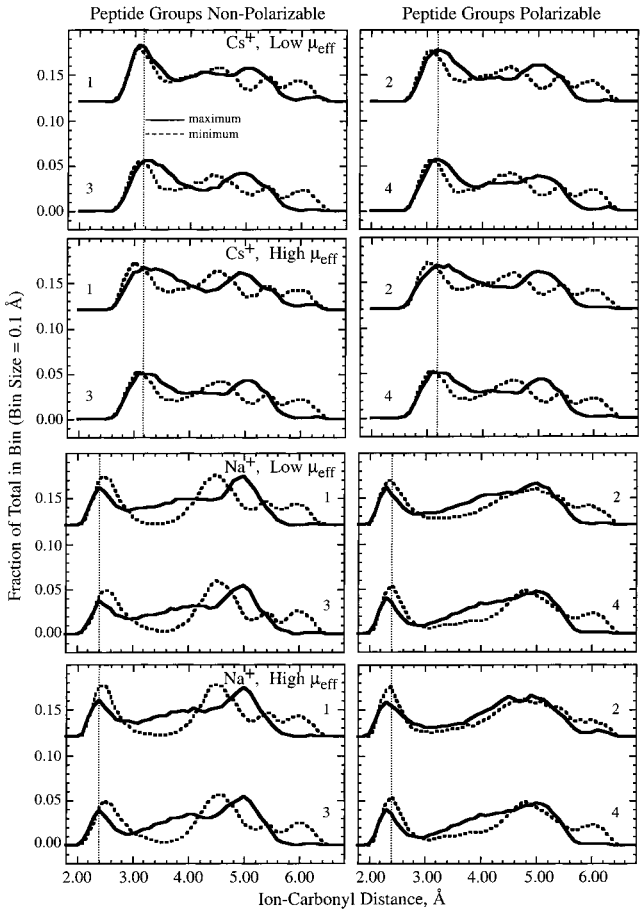

Figure 6. Ion−CO distances (in Å) for ions near energy extrema. The *x*-axis represents the distance; the *y*-axis, the fraction of the total found within the given bin. The upper pair has been translated vertically by 0.12 to simplify comparison. Shifts in the max/min distributions are associated with selective polarizability (see below).

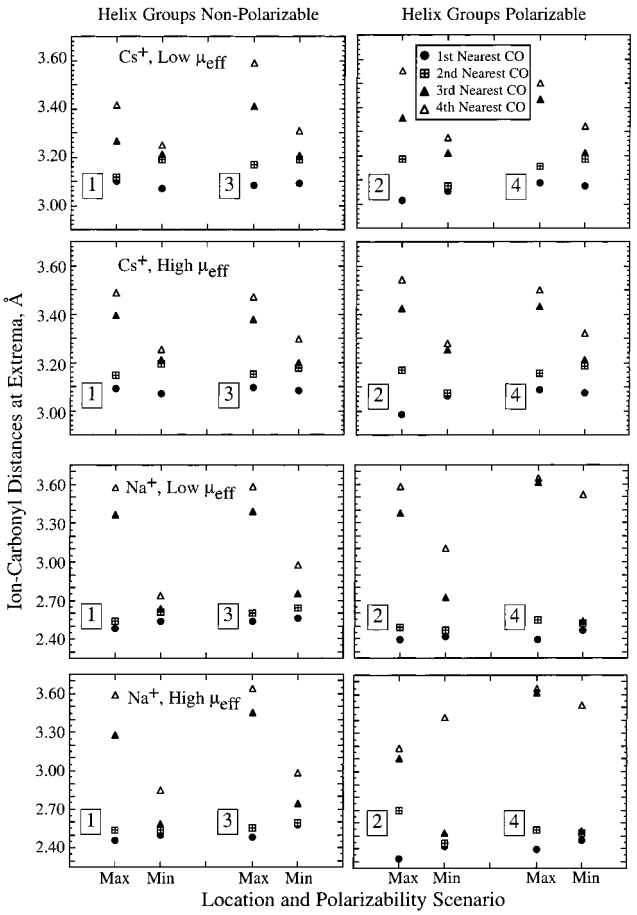

Figure 7. Average ion−carbonyl oxygen distances (in Å) in the vicinity of extrema for the highest and lowest energy barriers by category. RMS fluctuations: ∼0.10−0.25 Å, depending on proximity to ion.

matched nonpolarizable water scenarios by an average of 18%. Generally, CO coordination increases at high μ_{eff} with respect to low μ_{eff}.

Incorporating helix group polarizability tends to broaden the distributions for both cations, making them less sharply peaked. For cesium, the first maximum is broadened slightly more than the first minimum. For sodium, the effect is more dramatic; the clearly defined second peak at the maximum is broadened considerably when peptide groups are polarizable, even though those COs are located 5 Å or more from the ion.

Figures 7 and 8 illustrate ion−carbonyl and ion−water distances for the two polarizability scenarios in each grouping. The ions coordinate four carbonyls at both extrema. For cesium, two are closely coordinated at the maximum, whereas at the minimum, all four are closely coordinated. This correlates with the peak shift observed in Figure 6. Polarizable helix groups shorten the average distance for the first carbonyl ligands; polarizable water tends to expand these distances. Although the cesium ion can, and does, move off-axis in its trajectory through the channel, its greater size combined with the narrow channel diameter permits better solvation by the four closest carbonyls even when the Cs^+ is not centrally positioned in the $x-y$ plane of the window. From Figure 8 we see that ion−first water distances are uniformly shorter in the simulations in which barrier height is lower. For cesium, the first water is always closer to the ion at the minimum.

The coordination pattern for sodium differs slightly. At the maximum, sodium always coordinates two CO groups rather closely; at the minimum, that number rises to three, again consistent with peak shifts in the distributions (compare Figures 6 and 7). As with cesium, helix polarizability shortens the first ion−carbonyl distance, whereas polarizable water increases it. Ion−water distances are all shorter for the maximun−minimum pair that represents the lowest barrier height (Figure 8); unlike the case with cesium, however, with sodium the ion−first water distances are longer at the minimum than at the maximum.

Discussion

Conventional biomolecular force fields approximate various groups as having the same mean monomeric behavior. While acceptable for most structure-refinement applications or dynamics involving strictly neutral species, these force fields fail to adequately reflect local dynamics in the immediate vicinity of an ion. Recently, attempts have been made to refine these force fields to better approximate the channel environment by incorporating nonadditivity in the potential energy function, but only for ion−protein interactions.[22−24] Water is modeled in the conventional, approximate manner that reflects properties of the bulk liquid state. We consider this approach incomplete and prone to masking important channel behavior. Water, either in bulk or in the channel, is strongly polarized by the electric field of an ion. The local solvation environments are vastly different and the influence of polarization is very different in the two domains (the mean water dipole moments differ significantly). As has been stressed by various groups,[7,20,38] water should be treated as a polarizable species for correct evaluation of channel behavior. In part to highlight the

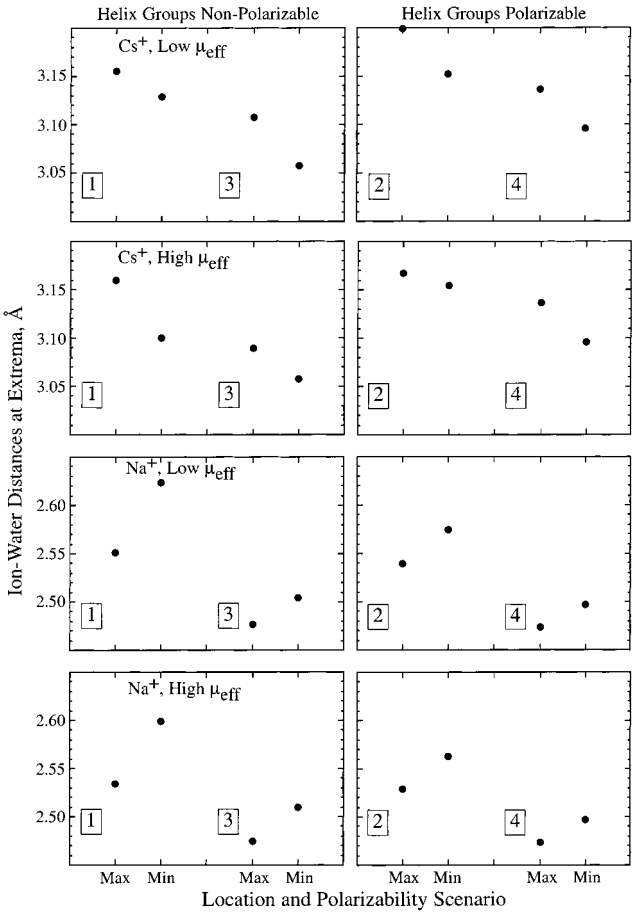

Figure 8. Average ion−water distances (in Å) in the vicinity of extrema for the highest and lowest energy barriers by category. RMS fluctuations: <0.10 Å.

importance of a full treatment of polarizability, we have undertaken the present study, comparing predictions made when polarizability is partially vs completely included or excluded in the potential function. Our analysis reveals the inadequacy of modeling that presumes channel water and bulk water can be described as equivalent fixed dipoles or that omits a full consideration of polarizability.

Water Structure in the Channel. We first examined how instantaneous readjustment of the magnitude of dipole moments of either water or peptide groups alters ion−water or water−water correlations relative to scenarios in which these quantities are fixed at mean values. Some early simulations of McKay et al.,[5] Skerra and Brickmann,[11] and Chiu et al.,[6,43] which focused particular attention on the nature of the channel water structure in the water-filled channel, employed potential functions in which groups possessed "average" properties and nonbonded interactions were approximated by a pairwise-additive energy term. In those simulations, water tended to maintain rather long-range correlations, despite the possibility of occasional gaps arising transiently in the single-file regime. Our results differ, regardless of polarizability scenario: The single-file water orientational distribution is bimodal, the water in the channel center being basically disoriented. Roux et al.[23] found similar behavior only when polarizability was incorporated; however, their water alignment was the opposite of ours. This suggests that water structure can be sensitive to the model details.[42,43] In our approach, based on purely dipolar CO groups, there is no explicit oxygen charge; this may limit the ability of carbonyls to form hydrogen bonds with water and thereby limit their orienting capacity.[43] Inclusion of the carbonyl quadrupole moment might be significant and could noticeably affect water correlations in the ion-free channel.

The most important single factor determining channel water structure is the size of the water dipole. High dipole moments promote ordering, as the waters interact primarily with the ion and with each other, rather than with the backbone. The limitations of a nonpolarizable treatment of water are most significant for waters close to the ion. Keeping the dipoles of the backbone group fixed raises the water dipole moments over that of the matched scenario, i.e., where all groups are polarizable (sc. 3 vs 4, Table 2). The fact that waters closest to the ion are more highly polarized by the electric field (an effect whose strength is related to cation identity) cannot be fully reproduced in systems where water is nonpolarizable.

Ion−water separations depend somewhat on the polarizability scenario (Table 3). Polarizable water tends to shorten the ion−first water distances for both ions. Polarizable peptide groups have an opposing effect for cesium, but a small complementary one for sodium. When backbone dipoles fluctuate, the sodium ion tends to move off-axis and coordinate strongly with two to three carbonyls. Given its small size, water is able, in this case, to move slightly closer to the ion, in a quasi-"back-door approach" from the side of the ion. Cesium, which is larger, cannot move far off-axis; tighter water coordination is not feasible. Consequently, when backbone dipoles fluctuate, the stronger interactions between CO ligands and Cs^+ push the waters back slightly, whereas for Na^+ the waters actually approach a bit closer. Beyond the first solvation shell, ion−water interactions are weakened for both ions when the backbone is polarizable, because the waters can interact more strongly with gramicidin. Transient gaps in the water chain are more frequent and larger when the helix dipoles fluctuate, presumably because of enhanced water−helix interaction distant from the ion. As expected, when water dipoles are fixed, the high-μ_{eff} category exhibits overall shorter ion−water distances.

Mean water−water separations, single-file water chain lengths, and location-specific water−water pair distances are all strongly influenced by partial or complete incorporation of polarizability. Polarizable water tends to strengthen water−water correlations, thereby reducing water−water distances both adjacent to and more distant from the ion. Polarizable helix groups tend to weaken water−water correlations by interacting more strongly with the ion, as well as by directly disrupting the single-file waters. In fact, the reason ion−water correlations beyond the first water sphere are uniformly weakened for polarizable helix scenarios is primarily perturbation of the water chain, although enhanced solvation of the ion by carbonyls may also play a minor role.

Polarizable backbone groups discourage the propagation of long-range ordering via dipolar coupling as measured by dipole vector orientations with respect to the channel axis, an effect that is more pronounced for cesium. The larger cation polarizes the waters less well than the smaller one, allowing greater interaction between the single-file waters and the peptide. Polarizable water opposes this tendency, favoring long-range angular correlation. This is attributable to the local, high water dipole moments. High, fixed dipole water moments foster greater correlation than does polarizable water.

We have identified important structural effects that appear when polarizability is selectively incorporated into the potential function. When water is made polarizable, then: (1) Ion−water distances shorten, especially for the small ion; (2) electrostriction (shorter water−water distances) is observed, also more notably for sodium; and (3) orientational correlation is retained with

sodium once again, exhibiting the greater correlation, being better able to polarize its neighboring groups. Allowing helix group dipoles to fluctuate has the opposite effect and with greater influence.

Internal Translocation Barrier Energetics. Trends that emerge from our PMF computations parallel those of the ion−water−helix correlations. Barriers are generally lower when helix dipole moments are fixed and higher when they are permitted to fluctuate. Making water polarizable has the opposite effect, resulting in the smallest barriers when peptide groups are fixed at average values while water dipoles fluctuate. With all groups polarizable, the tendency toward larger barriers resulting from enhanced peptide carbonyl−ion interactions is mitigated by stronger water−ion and water−water interactions. Interestingly, the low-μ_{eff} category, which was deliberately engineered to mimic mean electrostatic energetics, exhibits a broad range of barrier heights. This may be indicative of cooperative effects along the entire water chain, which arise only when polarizability is explicitly incorporated. Generally, a problem in channel permeation modeling is the serious overestimation of energy barriers with respect to experimentally derived estimates.[42] Our simulations reemphasize the need for complete treatment of polarization.[4,7,20] The largest barriers and greatest differences from the fully polarizable model appear when only backbone dipoles fluctuate.

Interestingly, in this context our most "realistic" force field is sc. 4, with an internal barrier for Na^+ movement of ∼2 kJ mol^{-1}. This value is similar to that deduced from a stochastic dynamics analysis of experimental data[44] and to that estimated by scaling the first Roux−Karplus profile[8] and fitting it to experiment by use of diffusion theory.[45]

Ionic Coordination. We have examined ionic coordination near the extrema. We looked at both the distributions and the average values for ion−carbonyl and ion−water distances for two reasons: (1) to identify different ionic coordination patterns associated with various polarizability scenarios, and (2) to examine whether scenario-specific coordination differences at extrema correlate with the trends in internal barrier heights. For both ions, traversing the barrier involves exchanging two carbonyls in the first coordination shell for two new carbonyls.

Although there is less overall close CO coordination for sodium than cesium, the scenario-specific differences in the sodium-occupied channel distributions are more striking. Cesium coordinates four CO groups at both the maximum and the minimum, whereas sodium is better coordinated at the minimum (three vs two close CO ligands). Generally, CO coordination increases when backbone group dipoles fluctuate and at high μ_{eff} (compared with low μ_{eff}). Water polarizability weakens ion−carbonyl group coordination with respect to nonpolarizable water, but not dramatically.

Incorporating helix group polarizability tends to eliminate some of the structure in the distributions for both cations, making them broader. For cesium, the first peak at the maximum is broadened slightly more than the corresponding peak at the minimum. For sodium, the effect is more dramatic; the clearly defined second peak at the maximum is broadened considerably when peptide groups are polarizable, even though those CO groups are located 5 Å or more from the ion. This suggests that cooperative effects may be important in determining barrier heights.

Coordination changes can rationalize the anomalous result that full polarizability (sc. 1 and 4) actually raises the barrier height for cesium but lowers it for sodium. The reason is interesting. Making helix groups polarizable raises energy barriers, since CO groups coordinate the ion more closely and waters are pushed back. Generally, allowing backbone group dipoles to fluctuate weakens ion−water and water−water correlations, but for sodium very close to the ion, the trend is reversed. As ion−carbonyl distances shorten, the sodium moves to the side of the channel and associates strongly with one or two carbonyls. Because the ion is small, water can now approach more closely from "behind" the ion and coordinate more effectively than in the nonpolarizable state, where water remains closer to the channel axis. Consequently, helix polarizability works to enhance very close ion−water coordination for sodium; for cesium, however, which stays closer to the axis, this does not occur. In general, the water chain behaves as an entity that assists the ion in moving between binding sites. In all our simulations with polarizable water and nonpolarizable backbone, the ion extensively sampled the region between the four solvating carbonyls. When the backbone was made polarizable with nonpolarizable water, the ion remained very tightly associated with two carbonyls throughout most of the simulation.

Summary

We have observed two distinct trends in our analysis. Making water polarizable causes channel water dipoles to increase, ion−water distances to shorten, and angular correlation to increase; in brief, ion−water correlations strengthen. Making backbone groups polarizable leads to increased ion−water and water−water distances, attenuated angular correlation, and diminished electrostriction; in sum, ion−helix correlations strengthen while ion−water and water−water correlations decrease. When no dipoles fluctuate, there is compensation, as the two effects of polarizability are basically opposed. An approximately similar effect is noted for internal barrier heights. Increased internal energy barriers map to differences in translocation-induced changes in ion−water and ion−carbonyl correlation. Barriers are generally higher when the backbone groups are polarizable, but lower when water is polarizable. When both groups and water are polarizable, the effects of helix polarizability generally predominate. Finally, we note that for many system properties, because the effects of water and backbone polarizability are antagonistic, computations neglecting polarization are often better than those utilizing partial treatment. Naturally, full incorporation of polarization effects is the preferred approach.

Acknowledgment. This work has been supported by a grant from the National Institutes of Health (GM-28643). We thank James K. Prater and Brian J. Cummings for providing computational resources and many helpful suggestions.

References and Notes

(1) Duca, K.; Jordan, P. C. *Biophys. Chem.* **1997**, *65*, 123.
(2) Fischer, W.; Brickman, J.; Läuger, P. *Biophys. Chem.* **1981**, *13*, 105.
(3) Pullman, A.; Etchebest, C. *FEBS Lett.* **1983**, *163*, 199.
(4) Lee, W. K.; Jordan, P. C. *Biophys. J.* **1984**, *46*, 805.
(5) MacKay, D. H. J.; Berens, P. H.; Wilson, K. R.; Hagler, A. T. *Biophys. J.* **1984**, *46*, 229.
(6) Chiu, S. W.; Subramaniam, S.; Jakobsson, E.; McCammon, J. A. *Biophys. J.* **1989**, *56*, 253.
(7) Åqvist, J.; Warshel, A. *Biophys. J.* **1989**, *56*, 171.
(8) Roux, B.; Karplus, M. *J. Am. Chem. Soc.* **1993**, *115*, 3250.
(9) Woolf, T. B.; Roux, B. *Proc. Natl. Acad. Sci. U.S.A.* **1994**, *91*, 11631.
(10) Finkelstein, A.; Andersen, O. S. *J. Membr. Biol.* **1981**, *59*, 155.
(11) Skerra, A.; Brickmann, J. *Biophys. J.* **1987**, *51*, 969.
(12) Roux, B.; Karplus, M. *Biophys. J.* **1991**, *59*, 961.
(13) Bogusz, S.; Busath, D. *Biophys. J.* **1992**, *62*, 19.

(14) Dorman, V.; Partenskii, M. B.; Jordan, P. C. *Biophys. J.* **1996**, *70*, 121.
(15) Partenskii, M. B.; Jordan, P. C. *J. Phys. Chem.* **1992**, *96*, 3906.
(16) Brooks, B. R.; Bruccoleri, R. E.; Olafson, B. D.; States, D. J.; Swaminathan, S.; Karplus, M. *J. Comput. Chem.* **1983**, *4*, 187.
(17) Hermans, J.; Berendsen, H. J. C.; van Gunsteren, W. F.; Postma, J. P. M. *Biopolymers* **1984**, *23*, 1513.
(18) Sun, H. *Macromolecules* **1995**, *28*, 701.
(19) Arsenio, J. L.; Martin-Pastor, M.; Jimenez-Barbero, J. *Int. J. Biol. Macromol.* **1995**, *17*, 137.
(20) Jordan, P. C. *Biophys. J.* **1990**, *58*, 1133.
(21) Lee, F. S., Chu, Z. T.; Warshel, W. *J. Comput. Chem.* **1992**, *14*, 161.
(22) Roux, B. *Chem. Phys. Lett.* **1993**, *212*, 231.
(23) Roux, B.; Prud′hom, B.; Karplus, M. *Biophys. J.* **1995**, *68*, 876.
(24) (a) Jorgensen, W. L.; Impey, R. W.; Chandrasekhar, J.; Madura, J. D.; Klein, M. L. *J. Chem. Phys.* **1983**, *79*, 926. (b) Woolf, T. B.; Roux, B. *Biophys. J.* **1997**, *72*, 1930.
(25) Arseniev, A. S.; Bystrov, V. F.; Ivanov, T. V.; Ovchinnikov, Y. A. *FEBS Lett.* **1985**, *186*, 168.
(26) Arseniev, A. S.; Barsukov, I. L.; Bystrov, V. F. In *Chemistry of Peptides and Proteins*; Ovchinnikov, Y. A.; Voelter, W.; Bayer, E.; Ivanov, T. V., Eds.; W. Voelter Co.: Berlin, 1986; Vol. 3, p 127.
(27) Cornell, B. S.; Separovic, F.; Baldassi, A. J.; Smith, R. *Biophys. J.* **1988**, *53*, 67.
(28) Nicholson, L. K.; Cross, T. A. *Biochemistry* **1989**, *28*, 9379.
(29) Ketchem, R. R.; Hu, W.; Cross, T. A. *Science* **1993**, *261*, 1457.
(30) Jordan, P. C. *J. Phys. Chem.* **1987**, *91*, 6582.
(31) Sung S. S.; Jordan P. C. *Biophys. J.* **1987**, *51*, 661.
(32) Roux, B.; Karplus, M. *J. Phys. Chem.* **1991**, *95*, 4856.
(33) Sawyer, D. B.; Koeppe, R. E.; Andersen, O. S. *Biochemistry* **1989**, *28*, 6571.
(34) Andersen, O. S.; Koeppe, R. E. *Physiol. Rev.* **1992**, *72*, S89.
(35) Killian, J. A. *Biochim. Biophys. Acta* **1992**, *1113*, 391.
(36) Koeppe, R. E.; Kimura, M. *Biopolymers* **1984**, *23*, 23.
(37) Jordan, P. C. In *Transport through Membranes, Carriers, Channels and Pumps*; Pullman, A.; Jortner, J.; Pullman, B., Eds.; Kluwer: Dordrecht, The Netherlands, 1988.
(38) Pangali, C. S.; Rao, M.; Berne, B. J. *J. Chem. Phys.* **1979**, *71*, 2975.
(39) Berendsen, H. J. C.; Postma, J. P. M.; van Gunsteren, W. F.; DiNola, A.; Haak, J. R. *J. Chem. Phys.* **1985**, *81*, 3684.
(40) Gear, C. W. *Numerical Initial Value Problems in Ordinary Differential Equations*; Prentice Hall: Englewood Cliffs, NJ, 1971.
(41) Evans, D. J.; Murad, S. *Mol. Phys.* **1977**, *34*, 32.
(42) Roux, B.; Karplus, M. *Annu. Rev. Biophys. Biomol. Struct.* **1994**, *23*, 731.
(43) Chiu, S. W., Jakobsson, E., Subramaniam, S.; McCammon, J. A. *Biophys. J.* **1991**, *60*, 273.
(44) Chiu, S. W.; Jakobsson, E. *Biophys. J.* **1987**, *52*, 33.
(45) McGill, P.; Schumaker, M. *Biophys. J.* **1996**, *71*, 1723.